Journal of Atmospheric and Ocean Science
Vol. 10, No. 4, December 2005, 361–375

Intrusions of warm and salty waters onto the NW and N Iberian shelf in early spring and its relationship to climate variability

G. GONZÁLEZ-NUEVO* and E. NOGUEIRA

Instituto Español de Oceanografía, Centro Oceanográfico de Gijón, Avda. Príncipe de Asturias 70bis, 33212-Gijón, Asturias, Spain

Temperature and salinity data from a series of cruises carried out on the NW and N Iberian shelf, between 1987 and 2005 during early spring, were analysed to investigate the inter-annual variability of the intrusions of warm and salty waters into the Cantabrian Sea, and its relationship with the meridional sea surface temperature (SST) gradient in the NE Atlantic and the main modes of climate variability affecting the Northern Hemisphere. A sub-surface front, that separates warmer and saltier (i.e. spicy) waters in the westernmost part of the Iberian shelf from the colder and fresher waters, characteristic of the easternmost part of the southern Bay of Biscay, was observed in all the analysed years. The location of this sub-surface front, which defines the limit of the influence of the Subtropical mode of Eastern North Atlantic Central Water ($ENACW_{st}$) advected by the Iberian Poleward Current (IPC), varied approximately between Finisterre Cape (43°N, 9°W) and Peñas Cape (43.5°N, 6°W), being located on average around the Ortegal Cape (43.5°N, 8°W). Its position, alongshore the Southern Bay of Biscay shelf, is displaced westward as the spring season progresses, and showed a positive correlation with the summer–autumn (July–October, JASO) meridional SST gradient (measured between 36°N 15°W and 46°N 15°W) of the previous year. This gradient was in turn correlated with the values of the Eastern Atlantic (EA) climate index for the same period.

Keywords: Iberian poleward current (IPC); Eastern North Atlantic Central Water (ENAWC); Spiciness; Sub-surface front; Bay of Biscay

1. Introduction

The NW and N Iberian shelf (between 42–45°N) is located in the inter-gyre zone that separates the subpolar and subtropical gyres of the North–East Atlantic (Pollard *et al*. 1996). The subpolar gyre is the formation area of the Eastern North Atlantic Central Water Subpolar mode ($ENACW_{sp}$), while to the south of the inter-gyre zone the formation of the Subtropical mode of this water mass ($ENACW_{st}$) (Pérez *et al*. 2001) takes place. These modes of central waters differ in their thermohaline characteristics being the subtropical, which are warmer and saltier, thus spicier (Flament 1986), than the subpolar mode waters (Ríos *et al*. 1992, Pérez *et al*. 1995).

*Corresponding author. Email: gonzalez_nuevo@gi.ieo.es

Journal of Atmospheric and Ocean Science
ISSN 1741–7538 print/ISSN 1741–7546 online © 2005 Taylor & Francis
http://www.tandf.co.uk/journals
DOI: 10.1080/17417530601127597

Fraga *et al*. (1981) found a subsurface front between the subtropical and subpolar modes of ENACW off Cape Finisterre (43°N, 9°W), and were the first to suggest a poleward advection of $ENACW_{st}$ along the Iberian margin. Their results were later confirmed by Pérez *et al*. (1993) using a biogeochemical approach. The presence of relatively warm and salty waters off NW Iberia has been noted since then by different authors (Pingree and Le Cann 1990, Ríos *et al*. 1992). These spicy waters enter into the Southern Bay of Biscay moving eastward along the Cantabrian continental shelf and slope (Pingree and Le Cann 1992, Bode *et al*. 2002, García-Soto *et al*. 2002).

This poleward flow, named Iberian Poleward Current (IPC) (Peliz *et al*. 2003), Portugal Coastal Counter Current (PCCC) (Ambar and Fiúza 1994, Álvarez-Salgado *et al*. 2003) or Navidad (Christmas) current (García-Soto *et al*. 2002), is a common feature of the winter circulation of eastern ocean margins (Neshyba *et al*. 1989) and has been described as a narrow, upper slope trapped current. Despite some controversy about the origin, extent and variability of the IPC (Peliz *et al*. 2005), it is generally accepted that the large-scale meridional density gradient, through the 'Joint Effect of Baroclinicity and Relief' (JEBAR) (Huthnance 1984, 1986, Pingree and New 1989) is the main driving mechanism of this poleward flow (Coelho *et al*. 1999). The effect of wind-stress is quantitatively less important (Peliz *et al*. 2003), but it may modify the flow, promoting its intensification and surfacing under poleward winds or its weakening of even reversal under equatorward winds (Haynes y Barton 1990, Álvarez-Salgado *et al*. 2003). According to Peliz *et al*. (2005), two aspects of the IPC that need to be investigated are the seasonality of the IPC, that is, the transition from winter (the development phase of the IPC according to these authors) to summer (decay phase), and the inter-annual variability and its relationship with the climate patterns affecting the North–East Atlantic.

We have analysed temperature and salinity data from CTD casts covering the NW and N Iberian shelf during spring (i.e. the transition from the development to the decay phase of the IPC) between the years 1987 and 2005. We have estimated the extension of the intrusion of warm and salty, thus spicy, waters characteristic of the IPC along the North Spanish shelf, and its relationship with the meridional sea surface temperature (SST) gradient on the NE Atlantic and the main modes of climate variability affecting the Northern Hemisphere.

2. Material and methods

2.1. *Database*

The hydrographic database is integrated by temperature and salinity data from CTD casts carried out on the NW and N Iberian shelf during spring (March–April) between the years 1987 and 2005 (table 1). The profiles were obtained in hydrographic stations distributed over the shelf and arranged in transects perpendicular to the coast (figure 1). Some of the hydrographic stations were visited up to 17 times during the analysed 18-year period. The profiles extend from the surface (5 m depth) down to 5 m above the bottom or to a maximum 200 m depth in deeper stations.

In order to investigate the relationship between the IPC and the meridional density gradient, which is considered the main forcing mechanism of this current (Peliz *et al*. 2005), we have used the time series of 4-months averaged SST difference

Table 1. Description of the cruises analysed (campaign, vessel and start and end date of the cruise).

Campaign	Vessel	Start	End
SARPAREA	Lura	13/04/87	24/04/87
MPHSARACUS	Cornide Saavedra	01/04/88	04/05/88
MPH	Investigador	18/04/90	09/05/90
ECOSARP	Cornide Saavedra	17/04/91	09/05/91
PROSARP	Cornide Saavedra	31/03/92	15/04/92
PROSARP	Cornide Saavedra	07/04/92	20/04/92
ICTIONORTE	Investigador	22/04/92	09/05/92
PELACUS	Cornide Saavedra	14/04/93	03/05/93
SEFOS	Cornide Saavedra	15/03/94	13/04/94
MPH	Cornide Saavedra	26/03/95	14/04/95
SEFOS	Cornide Saavedra	11/03/96	31/03/96
PELACUS	Thalassa	08/03/97	31/03/97
PELACUS	Thalassa	17/03/98	08/04/98
PELACUS	Thalassa	03/03/99	29/03/99
PELACUS	Thalassa	27/03/00	12/04/00
CAREVA	Cornide Saavedra	16/03/01	04/04/01
PELACUS	Thalassa	30/03/01	22/04/01
JUREVA	Cornide Saavedra	09/04/01	28/04/01
PELACUS	Thalassa	09/03/02	04/04/02
SAREVA	Cornide Saavedra	18/03/02	15/04/02
PELACUS	Thalassa	19/03/03	12/04/03
PELACUS	Thalassa	30/03/04	22/04/04
PELACUS	Thalassa	05/04/05	29/04/05

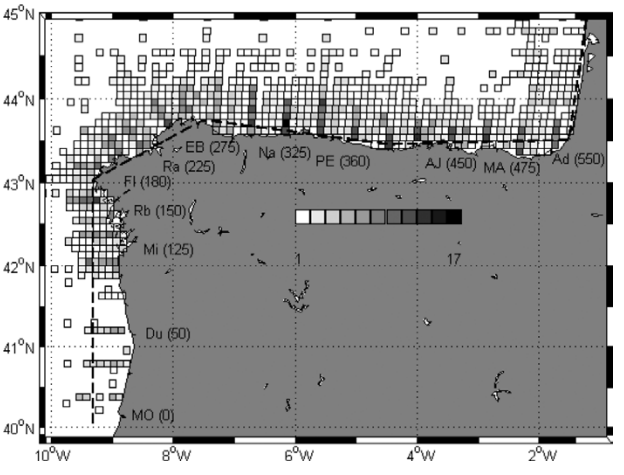

Figure 1. Position of the hydrographic stations in the different cruises used in this work (table 1). Each 'pixel' has a 25 nm^2 surface area. The grey scale represents the number of times each pixel was sampled during the 1987–2005 period. The black broken line parallel to the coast represents the trajectory used to refer the stations in relation to an along-shore axis. The principal geographic features are Mondego Cape (MO) (the arbitrary origin of the along-shore trajectory), Duero River (Du) Miño River (Mi), Rías Bajas (Rb), Finisterre Cape (FI), Rías Altas (Ra), Estaca de Bares Cape (EB), Nalón River (Na), Peñas Cape (PE), Ajo Cape (AJ), Machichaco Cape (MA), Adour River (Ad). The distance of the geographic features in the along-shore trajectory in relation to the arbitrary origin at Cape Mondego appear within brackets.

between 36°N 15°W and 46°N 15°W, calculated using NOAA_ERSST_V2 data provided by the NOAA/OAR/ESRL PSD, Boulder, Colorado, USA (http://www.cdc.noaa.gov/).

A set of climate indices, that prescribe the large-scale climatological patterns in the North Atlantic (Wallace and Gutzler 1981, Barnston and Lizevy 1987) was also used to assess its relationship with the inter-annual variability of the IPC (table 2). The monthly time series of these climate indices were obtained from the Climate Prediction Centre of the NOAA (http://www.cpc.ncep.noaa.gov/data/).

2.2. *Definition of the IPC front and its relationship with the SST meridional gradient and climate indices*

Due to the influence of continental land-masses, the thermohaline characteristics of shelf waters are much more variable than those of the oceanic realm. Consider for instance the cooling/heating of surface waters due to air temperature variability over land or the dilution effect associated with continental freshwater inputs. These processes modulate the temperature and/or salinity signatures of shelf waters, and thus may hinder the recognition of hydrodynamic processes on the basis of the analysis of thermohaline characteristics of surface waters (e.g. Bode *et al*. 2002).

We assume that the IPC front over the shelf separates bodies of water that are subject to a distinct influence of the Subtropical and Subpolar modes of ENACW: the southern–western side of the front is influenced by $ENACW_{st}$, while the northern–eastern side is influenced by $ENACW_{sp}$. According to this assumption, we analysed the change in the slope of the along-shelf transect of sub-surface (average values in the 70–80 m depth layer) spiciness (Flament 1986, 2002), which is a state variable derived from temperature and salinity data, and is most sensitive to isopycnal thermohaline variations. The analysis of this variable has been used to characterize intrusions of warm and salty waters associated with the California current system (Jackett and McDougall 1985, Lynn and Sympsom 1990). The procedure is schematized in figure 2 and an example of its application is given in figure 3. In these figures, we have denoted the limit of influence of spicy waters by the abbreviation IPC_f.

In order to investigate the relationship between the position of the IPC_f and the meridional SST gradient, we have conducted a lagged correlation analysis between the IPC_f, relative to a reference position located off Cape Mondego (41°N) (figure 1), and the time series of the 4-months averaged SST gradient. Later on, this SST gradient is related to the climate indices. Before the correlation analysis, the time series were detrended, if necessary, in order to make them stationary (Wei 1989). The time series were also tested for independence between successive time series values (i.e. autocorrelation) (Pyper and Peterman 1998) and normality.

3. Results

A sub-surface front separating the relatively warm and salty waters characteristic of the $ENACW_{st}$ and the fresher and colder waters characteristic of $ENACW_{sp}$ was found in all the studied cruises (figure 4). The position of the IPC_f associated with the $ENACW_{st}$ in the Southern Bay of Biscay shelf oscillated between Finisterre Cape, (43°N 9°W) and Peñas Cape (43.5°N 6°W) (i.e. 180 and 360 nm along-shore distance

Table 2. Definition and effects on temperature and effects on precipitation (i.e. surface salinity) of the main climate patterns of the Northern Hemisphere (modified from Climate Prediction Centre of the NOAA: http://www.cpc.ncep.noaa.gov/data/).

Pattern	Description	Effects on surface temperature	Effect on precipitation
North Atlantic Oscillation (NAO)	North–South dipole: one centre located over Greenland and the other of the opposite sign spanning central latitudes of the North Atlantic (35°–40° N).	• Eastern US and across northern Europe. • Greenland and across southern Europe and the Middle East.	• Northern Europe and Scandinavia in winter. • Southern and central Europe.
East Atlantic (EA)	North–south dipole. Anomaly centres spanning the North Atlantic from east to west. The anomaly centres of the EA pattern are displaced south-eastward to the approximate nodal lines of the NAO pattern.	• Europe in all months. • Southern US during January-May and in the north-central US during July–October.	• Northern Europe and Scandinavia. • Southern Europe.
Scandinavian (SCAN)	A primary circulation centre over Scandinavia, with weaker centres of opposite sign over western Europe and eastern Russia/western Mongolia.	• Russia and western Europe. I.	• Central and southern Europe. • Scandinavia.
East Atlantic Western Russia (EA/WR)	Two positive height anomalies located over Europe and northern China, and negative height anomalies located over the central North Atlantic and north of the Caspian Sea.	• Eastern Asia. • Western Russia and Northeastern Africa.	• Eastern China. • Central Europe.
Polar/Eurasian (POL)	A negative height anomalies over the polar region and positive anomalies over northern China and Mongolia.	• Eastern Siberia. • Eastern China.	• Polar region north of Scandinavia.
West Pacific (WP)	Winter and spring: north-south dipole of anomalies (Kamchatka Peninsula and south-eastern Asia and western subtropical North Pacific). These anomalies exhibit a strong northward shift from winter to summer.	• Lower latitudes of the western North Pacific in winter and spring. • Eastern Siberia in all seasons.	• High latitudes of the North Pacific. • Central North Pacific especially during the winter and spring.
Pacific/North America (PNA)	Positive heights in Hawaii and over the intermountain region of North America, negative heights located south of the Aleutian Islands and over the southeastern US.	• Western Canada and US. • South-central and southeastern US.	• Gulf of Alaska North–western US. • Midwestern US.

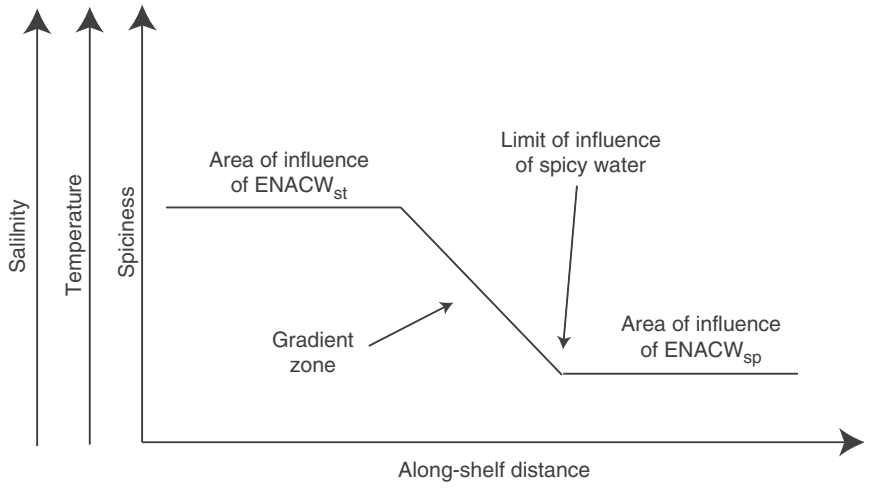

Figure 2. Schematic representation of the interaction of relatively warmer and saltier ENACW$_{st}$ and the relatively colder and fresher ENACW$_{sp}$. The IPC$_f$ is the point where the slope of the along-shore spiciness value tends to zero.

from Mondego Cape, respectively). The average position of the IPC$_f$ was located around Ortegal Cape (43.5°N 8°W) (i.e. 300 nm from Mondego Cape).

The typology of the averaged 70–80 m depth along-shore spiciness values varied from year-to-year (figure 4). For instance, some years showed higher values of spiciness than the mean distribution estimated for the 1987–2005 time series (i.e. Pelacus 1997, 1993), while other years exhibited lower values than the mean distribution (i.e. Pelacus 2003, 2005). In some cases we observed a departure from the general frontal structure defined in figure 2. For instances, the cruises MPH 1990 and Sefos 1996 showed an increase of the spiciness values in the eastern part of IPC$_f$, while in Pelacus 2002, Sareva 2002 and Pelacus 2005 cruises, the coastal-offshore variation of the data (i.e. the vertical axis of the graphs from a given along-shore position) between Finisterre Cape and Ajo Cape (relative along-shore distance 180 and 450 nm respectively) was higher than for the rest of the cruises.

However, since all the analysed cruises were carried out at different times during spring (table 1), we have considered the possible effect of the short-term scale (i.e. intra-seasonal) variability of the IPC$_f$. The estimated value of the IPC$_f$ and the start week of each cruise were negatively correlated, which denotes the reduction of the influence of the ENACW$_{st}$ in the Cantabrian Sea as the season progresses. We used the linear regression model that captures this relationship (IPC$_f = -11.04$ Week $+ 450$; $n = 22$, $r = 0.42$, $\alpha < 0.05$) to correct the effect of this intra-seasonal variability before analysing the inter-annual variability of the IPC$_f$ and its relationship with the meridional SST gradient. Thus, the position of the IPC$_f$ was recalculated as if all the cruises were sampled in the first week of March (i.e. the earliest start date of all the analysed cruises, table 1) (figure 5).

The time series of the IPC$_f$ showed a significant positive linear trend. The IPC$_f$ displaced eastward at a rate of 4.41 nm year^{-1} ($n = 18$, $r = 0.55$, $\alpha < 0.01$). The increase of the penetration of relative warm and salty waters into the Cantabrian Sea is not related with an increase of the mean values of spiciness measured in the whole area. Thus, some years (e.g. MPH 1990 cruise) showed high values of spiciness

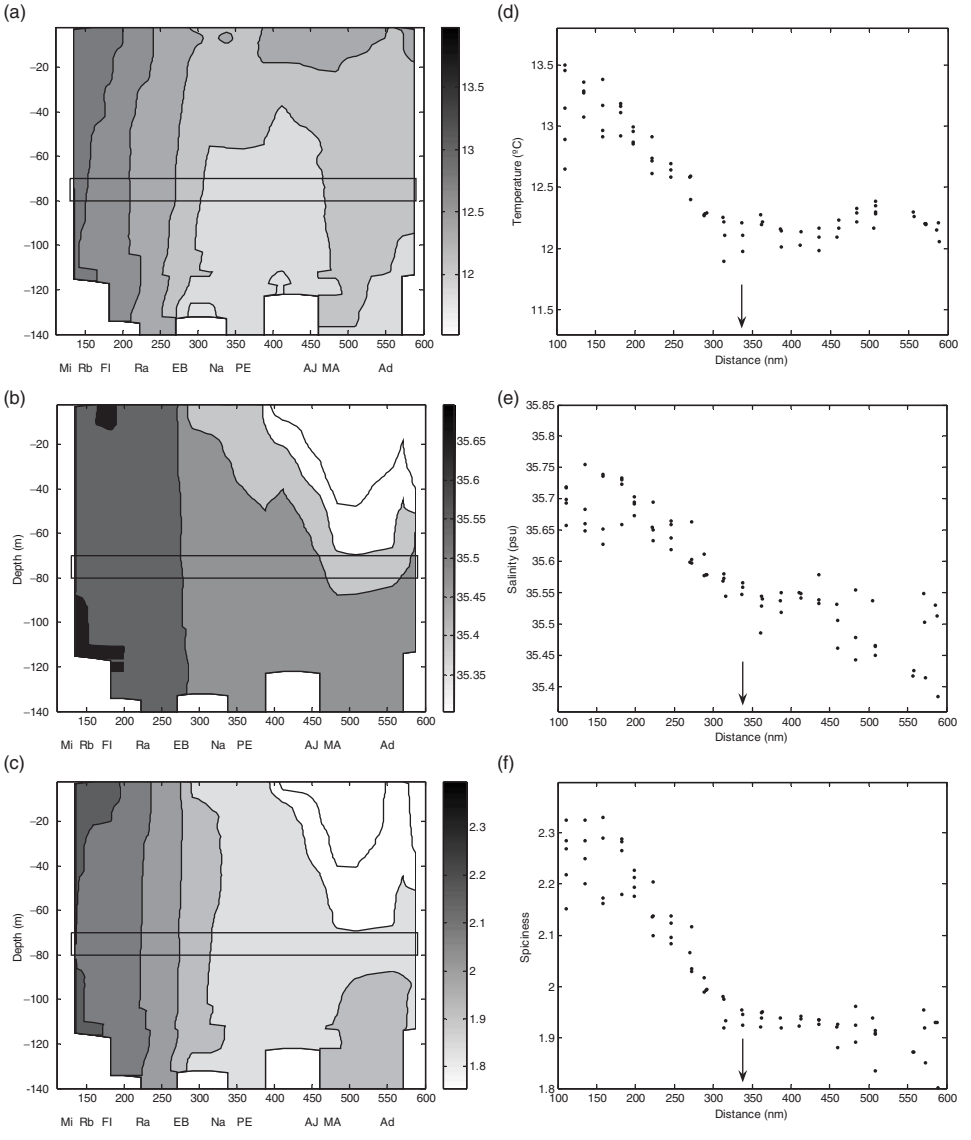

Figure 3. Along-shore section of the Pelacus 2004 cruise for (a) temperature, (b) salinity and (c) spiciness. These contour plots were done using the stations nearest to the coast with more than 100 m depth. Mean values of the 70–80 m depth layer of (d) temperature, (e) salinity and (f) spiciness in the along-shore trajectory for all the hydrographic across-shelf stations. The arrows represent the position of the IPC_f.

but lower values of the IPC_f (i.e. less penetration of spicy waters into the Cantabrian Sea) (figure 4). This result is a consequence of the method used to calculate the IPC_f, which is based on relative differences of spiciness between western and eastern locations rather than on absolute values, and thus the differences of the IPC_f are not necessarily linked to an increment of the spiciness value in the whole area.

Assuming that the meridional density gradient generated principally by temperature is the main forcing mechanism of the IPC (Peliz *et al.* 2005),

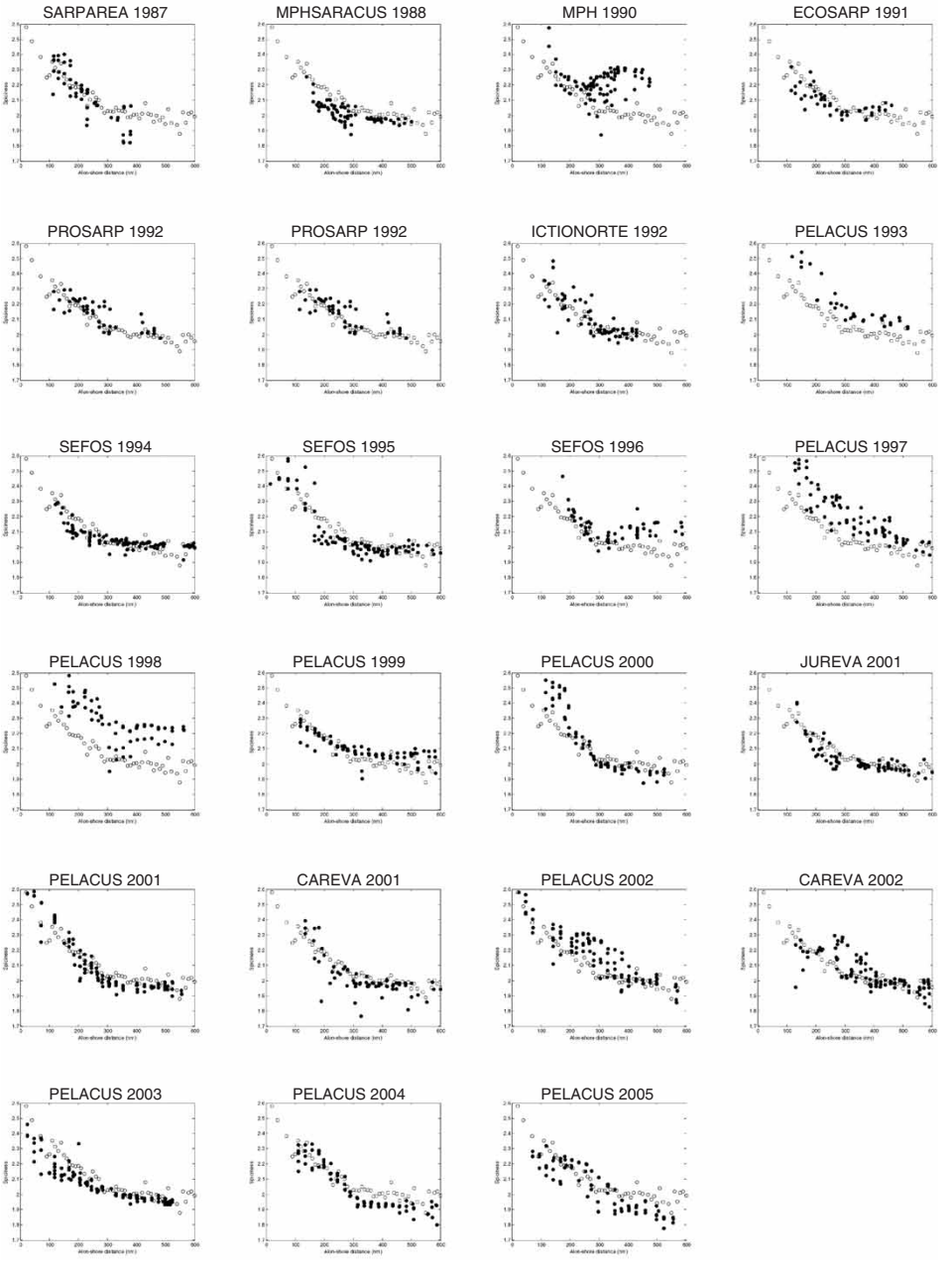

Figure 4. Distributions of the mean values of the 70–80 m depth layer of spiciness for all the cruises analysed (Black dots). The white circles represent the mean distribution calculated using all the cruises (1987–2005).

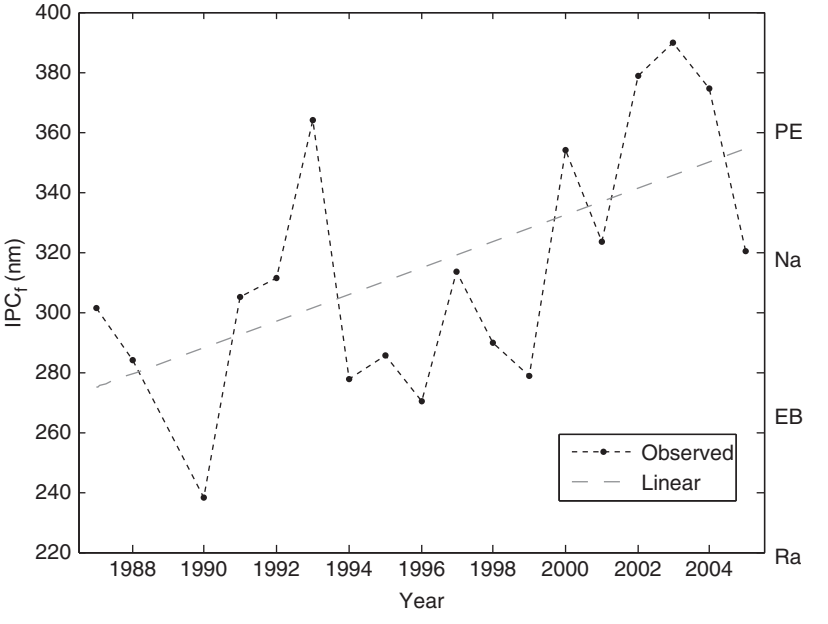

Figure 5. Time series of the position of the IPC_f, corrected for the effect of intra-seasonal variability. The IPC_f of the years with more than one cruise (table 1) is the mean of the different cruises within this year. The black broken line represents the linear trend of the observed values of IPC_f. The principal geographic features in the second *Y* axis are marked (see caption of figure 1).

we performed a lagged correlation analysis between the IPC_f (corrected to remove the intra-seasonal variability and detrended) and the meridional SST gradient between 36°N 15°W and 46°N 15°W. Both time series showed a significant positive correlation at lag 6 (July–October, JASO) for the non-parametric Kendall and Spearman correlation coefficients but not for the parametric Pearson correlation coefficient (table 3). Since the Pearson correlation coefficient evaluates the linear correlation while the other non-parametric correlations coefficients consider other kinds of relationships that depart from linearity, the estimated correlation values suggest a positive non-linear relationship between the IPC_f and the meridional SST gradient.

For the summer-autumn period (JASO), the results of the correlation analysis between the meridional SST gradient and the climate indices are shown in table 4. Only the (detrended) Eastern Atlantic (EA) index showed a significant correlation with the meridional SST gradient.

4. Discussion

The principal mechanism for advection of warm and salty waters in the Cantabrian Sea was the IPC. The dynamics of this current in spring has not been well described. The negative relationship between the IPC_f and the week of the year reflects the weakening of the current as the spring season progresses, thus capturing the reduced influence of spicy waters into the Cantabrian shelf towards the summer. This result

Table 3. Parametric Pearson and non-parametric Spearman and Kendall correlation coefficients between the IPC_f (corrected to filter out the short-term variability and detrended) and the 4-months averaged meridional SST gradient for the first 12 lags (lag 0 corresponds to the period January–April). Significant coefficients at 0.05 probability level are marked by '*'.

Lag	Pearson	Spearman	Kendall
0	0.06	−0.14	−0.09
1	0.03	−0.05	−0.03
2	0.01	0.02	0.03
3	0.00	0.11	0.09
4	0.01	0.10	0.07
5	0.04	0.34	0.26
6	0.09	0.42*	0.34*
7	0.06	0.38	0.27
8	0.03	0.22	0.14
9	0.00	0.10	0.12
10	0.10	−0.31	−0.22
11	0.13	−0.30	−0.22
12	0.15	−0.31	−0.24

Table 4. Linear trend of each climate index, and Pearson, Spearman and Kendall correlation coefficients between the latitudinal SST gradient and the climate modes for the period July–October (JASO).

Pattern	Trend	Pearson	Spearman	Kendall
EA	0.016*	0.10*	0.29*	0.18*
EA/WR	−0.009	0.00	0.01	0.01
NAO	0.000	0.02	−0.11	−0.08
PNA	−0.005	0.04	0.16	0.10
POL	0.004	0.00	−0.03	−0.03
SCAN	−0.002	0.01	0.01	0.01
WP	0.000	0.05	0.17	0.12

reinforces the hypothesis on the dynamics of the IPC described by Peliz (Peliz *et al.* 2005), who suggested that the annual evolution of the current present two phases: the development phase and the decay phase. The development phase occurs during late-fall and winter as a consequence of the strengthening of the meridional density gradient. The decay phase occurs in late-winter and early-spring, and the main process that dominates this phase is the weakening of the meridional density gradient and the erosion of the near surface structure by the action of wind stress and the interactions with the mesoscale eddy field.

The positive correlation found between the IPC_f time series and the meridional SST gradient from July to October (JASO) of the previous year supports the role of the meridional density gradient as the driving mechanism of the IPC during the development phase in the summer-autumn transition. As is illustrated the seasonal cycle of the meridional SST gradient (figure 6) during the summer-autumn transition increases from 3.5°C in July to 4.6°C in October (figure 6), after which it decreases at a slower rate from November to July.

However, the observed relationship between the EA index and the meridional SST gradient during the summer-autumn transition (JASO) may capture the

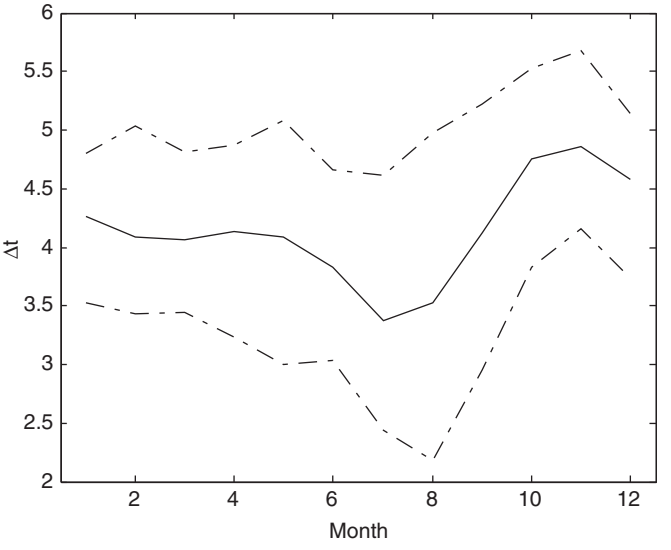

Figure 6. Seasonal cycle of meridional SST gradient calculated using NOAA_ERSST_V2 data from 1950 to 2005 provided by the NOAA/OAR/ESRL PSD, Boulder, Colorado, USA, from their web site at http://www.cdc.noaa.gov/. The upper and lower broken lines represent the maximum and minimum values of each month, respectively.

atmosphere–ocean interaction. In this part of the year, the positive values of the EA index indicate an intensification of the subtropical ridge and the North Atlantic low, giving rise to the formation of a strong North–South dipole in the North–East Atlantic (figure 7a). This atmospheric pressure configuration could generate a stable situation in the subtropical areas, which may favour the warming of the sea surface by means of solar irradiance. This hypothesis is supported by the positive correlation between the EA pattern and the atmospheric surface temperature in these latitudes (figure 7b).

The results presented here, based on the use of the IPC_f as an index to monitor the relevance of the intrusions of $ENACW_{st}$ into the Cantabrian Sea, contrasted to some extent with other estimations of the intensity of the IPC. Peliz *et al.* (2005) calculated an IPC intensity index using the difference of satellite-derived SST between coastal (40°N 14°W) and ocean locations (40°N 9–10°W) from 1985 to 2001. Using this index, these authors found three periods of high intensity of the IPC: 1989–1990, 1996–1998 and 2001. Garcia-Soto *et al.* (2002) using another index based on the satellite-derived SST differences between 8°W and 4°W in the Cantabrian Sea, reported also that the years 1996 and 1998 (but not 1997) corresponded with a strong poleward flow, and found also a significant linear correlation between the SST index they have defined and the winter NAO. This result was obtained after selecting visually the years with a strong IPC signal (i.e. high values of SST along the Iberian shelf).

The inter-annual variability of the limit of influence of warm and salty waters (i.e. the IPC_f) advected by the IPC derived from the sub-surface spiciness values, did not show exactly the same pattern, although the years of strong poleward flow pointed out by Peliz *et al.* (2005) had higher values of spiciness all over the shelf than the mean value calculated from 1987 to 2006 (figure 4). González-Pola *et al.* (this issue),

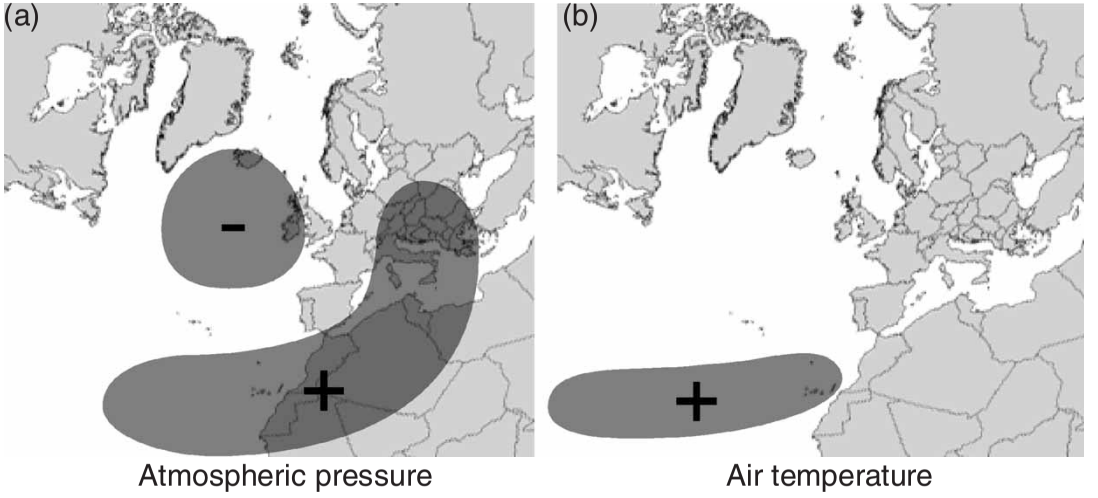

Figure 7. Correlations between the positive phase of the EA pattern with (a) the atmospheric pressure field and (b) the air temperature at sea level in the Northern Hemisphere during the autumn. Positive correlations areas are marked with '+' and negative correlations areas are marked with '–' (figure modified from Climate Prediction Centre of the NOAA http://www.cpc.ncep.noaa.gov/data/).

using an analysis based on *in situ* thermohaline data suggest that 2002 was also a year with a strong poleward flow. This result is in accordance with our findings, since this year presented the second highest value of the IPC_f for the analysed period.

The differences between the results presented here and those from other authors could be related with the definition of the various indices utilized and the source data used for its calculation (i.e. in-the-field or satellite-derived surface data). Peliz *et al*. (2005) calculated a surface index from January to February using satellite-derived SST data; while Garcia-Soto *et al*. (2002) produced their index from winter remote sensing-derived SST. In contrast, the IPC_f defined here was calculated using in-the-field sub-surface (averaged between 70 m and 80 m depth) data, acquired during spring (i.e. during the decay phase of the IPC rather than in the development phase). Thus, the different indices characterize different situations and phases of the IPC development, so the comparison among indices is not straightforward. On the other hand the interpretation of the relationship between NAO and the gradient in the Cantabrian Sea found by Garcia-Soto (Garcia-Soto *et al*., 2005) is complicated. We have not found a significant relationship between the NAO index and the meridional SST gradient. The atmospheric pressure configuration of the NAO it pattern generates a north-south dipole similar to the EA pattern structure, but in the case of the NAO is displaced north-westerly, which may probably diminish the capacity to generate the meridional SST gradient necessary to force the dynamics of the IPC.

The increasing trend of the IPC_f that we have found in the analysed period (1987–2005) and its relationship with ocean features and the atmospheric climate processes have important implications since it may influence the development of plankton and pelagic communities in a critical part of the annual production cycle, influencing for instance the spatial distribution of different ecosystem components. The impact of the intrusions of $ENAWC_{st}$ into the Cantabrian Sea has been investigated in relation to the distribution of picoplankton (Morán *et al*., submitted), phytoplankton (Bode *et al*. 2002), zooplankton (Cabal *et al*. 2006), sardine eggs (Baldó and Bernal, per. com.) or fish populations (Sánchez and Gil 2000). Thus, better understanding of the mechanisms that modulate the dynamics of the IPC during its decay phase are desirable in order to improve the management of the ecosystem (FAO 2003).

5. Conclusions

The influence of warm and salty waters advected by the IPC into the Cantabrian Sea during the winter-spring transition is a process that was observed in all the cruises analysed, which generated a subsurface front that varied its position from year to year.

The penetration of the IPC presented two levels of variability. Short-term scale variability (i.e. intra-seasonal) in the winter-spring transition, which translates in a decreasing influence of spicy waters in the Cantabrian Sea as the spring season progresses, and a large-scale, inter-annual variability, represented by an increasing trend that produced an eastward displacement of the IPC_f of 100 nm in the last two decades.

The position of the IPC_f is positively correlated with the latitudinal SST gradient measured from July to October (JASO) of the previous year. This SST gradient seems

to be the principal factor of the IPC dynamics. The north–south SST gradient was positively correlated with the EA during this part of the year (JASO).

Acknowledgements

The authors would like to thank all people that collaborated in the cruises and in the processing of all the data used in this work. Special thanks to Rafael Revilla for its help in the preparation of figures. We also acknowledge the comments of the referees that greatly improved the quality of the manuscript. G. G-N is a recipient of a pre-doctoral fellowship from the 'Consejería de Educación y Cultura del Principado de Asturias'.

Bibliography

Álvarez-Salgado, X.A., Figueiras, F.G., Pérez, F.F., Groom, S., Nogueira, E., Borges, A.V., Chou, L., Castro, C.G., Moncoiffé, G., Ríos, A.F., Miller, A.E.J., Frankignoulle, M., Savidge, G. and Wollast, R., 2003, The Portugal coastal counter current off NW Spain: new insights on its biogeochemical variability. *Progress in Oceanography*, **56**, pp. 281–321.

Ambar, I. and Fiuza, A., 1994, Some features of the Portugal Current System: a poleward slope undercurrent, an upwelling related southward flow and an autumn-winter poleward coastal surface current, *2nd International Conference on Air-Sea Interaction & on Meteorology & Oceanography of the Coastal Zone*, preprints, American Meteorological Society, September 22–27, pp. 286–287.

Barnston, A.G. and Livezey, R.E., 1987, Classification, seasonality and persistence of low-frequency atmospheric circulation patterns. *Monthly Weather Review*, **115**, pp. 1083–1126.

Bode, A., Varela, M., Casas, B. and González, N., 2002, Intrusions of eastern North Atlantic central waters and phytoplankton in the north and northwestern Iberian shelf during spring. *Journal of Marine Systems*, **36**, pp. 197–218.

Cabal, J., González-Nuevo, G. and Nogueira, E. 2006 Hydrographic conditions and mesozooplankton species distribution in the Bay of Biscay shelf during spring 2004. In *Special Volume on the X International Symposium on Oceanography of the Bay of Biscay*, F. Vilas, B. Rubio, J.B., Diez, G. Francés, A.M. Bernabeu, E. Fernández, D. Rey and G. Rosón (Eds).

Coelho, H.S., Neves, R.R., Leitao, P.C., Martins, H. and Santos, A.P., 1999, The slope current along the western European margin: a numerical investigation. *Boletín del Instituto Español de Oceanografía*, **15**(1–4), pp. 61–72.

FAO, 2003. La Ordenación Pesquera. 2. El enfoque de ecosistemas en la pesca. FAO Orientaciones Técnicas para la Pesca Responsable. Vol. 4, Supl. 2. p. 133 (Roma: FAO).

Flament, P., 1986, Fine structure and subduction associated with upwelling filaments, PhD dissertation, University of California at San Diego.

Flament, P., 2002, A state variable for characterizing water masses and their diffusive stability: spiciness. *Progress in Oceanography*, **54**, pp. 493–501.

Fraga, F., 1981, Upwelling off the Galician coast, Northwest Spain. In *Coastal Upwelling. Coastal and Estuarine Science*, F.A. Richards (Ed.), Vol. 1, pp. 176–182 (Washington, DC: AGU).

García-Soto, C., 2002, Navidad development in the southern Bay of Biscay: climate change and swoddy structure from remote sensing and *in situ* measurements. *Journal of Geophysical Research*, **107**, pp. 1–29.

Haynes, R. and Barton, E.D., 1990, A poleward flow along the Atlantic coast of the Iberian Peninsula. *Journal of Geophysical Research*, **95**, pp. 11425–11441.

Huthnance, J.M., 1984, Slope currents and 'JEBAR'. *Journal of Physical Oceanography*, **14**, pp. 795–810.

HUTHNANCE, J.M., 1986, The subtidal behaviour of the Celtic Sea 3: a model of shelf waves and surges on a wide shelf. *Continental Shelf Research*, **5**, pp. 347–377.

JECKETT, D.R. and MCDOUGALL, T.J., 1985, An oceanographic variable for the characterisation of intrusions and water masses. *Deep-Sea Research*, **32**, pp. 1195–1207.

LYNN, R.J. and SIMPSOM, J.J., 1990, The flow of the undercurrent over the continental borderland off southern California. *Journal of Geophysical Research*, **95**, pp. 12995–13008.

MORÁN, X.A.G., BODE, B., SUÁREZ, L.A. and NOGUEIRA, E. Relationship between cell-specific nucleic acid content and activity of heterotrophic bacteria in temperate shelf waters. *Aquatic Microbial Ecology*, in press.

NESHYBA, S.J., MOOERS, C.N. K, SMITH, R.L. and BARBER, R.T., 1989, Poleward flows along eastern ocean boundaries. *Springer-Verlag Coastal and Estuarine Studies*, **34**, p. 374.

PELIZ, A., DUBERT, J., HAIDVOGEL, D.B. and LE CANN, B., 2003, Generation and unstable evolution of a Density-Driven Eastern Poleward current: the Iberian Poleward current. *Journal of Geophysical Research*, **108**, .

PELIZ, A., DUBERT, J., SANTOS, A.M.P. and LE CANN, B., 2005, Winter upper ocean circulation in the Western Iberia Basin. Fronts, Eddies and Poleward flows: an overview. *Deep-Sea Research I*, **52**, pp. 621–646.

PÉREZ, F.F., MOURIÑO, C., FRAGA, F. and RÍOS, A.F., 1993, Displacement of water masses and remineralization rates off the Iberian Peninsula by nutrient anomalies. *Journal of Marine Research*, **51**, pp. 869–892.

PÉREZ, F.F., RÍOS, A.F., KING, B.A. and POLLARD, R.T., 1995, Decadal changes of the 0–S relationship of the Eastern North Atlantic Central Water. *Deep–Sea Research II*, **42**, pp. 1849–1864.

PÉREZ, F.F. and CASTRO, C.G., 2001, Coupling between the Iberian basin - scale and the Portugal boundary current system: a chemical study. *Deep-Sea Research I*, **48**, pp. 1519–1533.

PINGREE, R.P. and NEW, A.L., 1989, Downward propagation of internal tidal energy into the Bay of Biscay. *Deep–Sea Research*, **36**, p. 735.

PINGREE, R.D. and LE CANN, B., 1990, Structure, strength and seasonality of the slope currents in the Bay of Biscay. *Journal of Marine Biology Association. U.K*, **70**, pp. 857–885.

PINGREE, R.D. and LE CANN, B., 1992, Three anticyclonic slope water oceanic eddies (swodies) in the southern Bay of Biscay in 1990. *Deep-Sea Research*, **39**, pp. 1147–1175.

POLLARD, R.T., GRIFFITHS, M.J., CUNNINGHAM, S.A., READ, J.F., PÉREZ, F.F. and RÍOS, A.F., 1996, Vivaldi 1991-A study of the formation, circulation and ventilation of Eastern North Atlantic Central Water. *Progress in Oceanography*, **37**, pp. 167–192.

PYPER, B.J. and PETERMAN, R.M., 1998, Comparison of methods to account for autocorrelation in correlation analyses of fish data. *Canadian Journal of Fisheries and Aquatic Sciences*, **55**, pp. 2127–2140.

RÍOS, A.F., PÉREZ, F.F. and FRAGA, F., 1992, Water masses in the upper and middle North Atlantic Ocean east of the Azores. *Deep-Sea Research*, **39**, pp. 645–658.

SÁNCHEZ, F. and GIL, J., 2000, Hydrographic mesoscale structures and Poleward Current as a determinant of hake (Merluccius merluccius) recruitment in the southern Bay of Biscay. *ICES Journal of Marine Science*, **57**, pp. 152–170.

WALLACE, J.M. and GUTZLER, D.S., 1981, Teleconnections in the geopotential height field during the Northern Hemisphere winter. *Monthly Weather Review*, **109**, pp. 784–812.

WEI, W.W.S., 1989, Time series analysis. Addison-Wesley Publishing Company, ISBN 0-201-15911-2, p. 478.